IEEE Access
Multidisciplinary | Rapid Review | Open Access Journal

Received January 29, 2021, accepted February 15, 2021, date of publication February 22, 2021, date of current version March 3, 2021.

Digital Object Identifier 10.1109/ACCESS.2021.3060995

Characterization of Radio Signal Strength Fluctuations in Road Scenarios for Cellular Vehicular Network Planning in LTE

MATÍAS TORIL[1], VOLKER WILLE[2], SALVADOR LUNA-RAMÍREZ[1], MARIANO FERNÁNDEZ-NAVARRO[1], AND FERNANDO RUIZ-VEGA[1]

[1]Departamento de Ingeniería de Comunicaciones, Universidad de Málaga, 29010 Málaga, Spain
[2]Nokia, Huntingdon CB23 6DP, U.K.

Corresponding author: Matías Toril (mtoril@ic.uma.es)

ABSTRACT Road coverage will be a key issue for the success of connected car applications. In this work, a comprehensive analysis of radio signal strength fluctuations on roads in a Long Term Evolution (LTE) system is presented. For this purpose, a measurement campaign based on drive tests was carried out to assess the coverage levels that can be expected on ordinary roads by normal in-car terminals in a country of the European Union. Measurements were collected on 1,000 km of road by 2 vehicles covering the same route. By comparing signal level samples at the same geographical location, taken at slightly different times, a statistical model of fluctuations is derived. Then, the impact of different factors (e.g., shadowing, environment, handover, etc.) on the signal level received from the serving cell is assessed. Results show that large deviations of signal level (up to 23 dB) are observed at the same geographical location.

INDEX TERMS Coverage, propagation, fading, measurement, drive test, road, network planning, cellular vehicle to everything (C-V2X), statistical model.

I. INTRODUCTION

In recent years, ''connected car'' has emerged as a key use case for 5G communication systems [1]. Its ability to increase road safety, reduce environmental impact and improve traffic management have long attracted the attention of both the telecommunication and the automotive sectors [2], [3]. By 2025, it is expected that the number of connected cars in operation will be hundreds of millions [4]. These expectations have stimulated research and standardization activity on the topic. As a result, the latest cellular standards (e.g., Third-Generation Partnership Project Release 14 [5] and Release 16 [6]) have been designed with connected car in mind.

Based on existing standards, future cellular systems will allow information exchange from vehicles to other vehicles (V2V), to communication networks (V2N), to road infrastructure (V2I) and to pedestrians (V2P). Thus, cars will share positions and sensor measurements, while receiving information from surrounding infrastructure. The range of services supported will include regulated Cooperative Intelligent Transport Systems (C-ITS), Advanced Driver Assistance Systems (ADAS), connected road infrastructure services, vehicle-centric Original Equipment Manufacturers (OEM) telematics, fleet management and infotainment [7].

For the above to become a reality, several challenges must still be addressed. Road safety and autonomous driving impose strict requirements in terms of latency and link availability, hard to achieve in mobility scenarios [8]. To satisfy them, a combination of radio access and networking techniques have been proposed as key technology enablers (e.g., millimeter waves [9], non-orthogonal multiple access [10], link adaptation [11], joint resource allocation [12], network slicing [13], mobile edge computing [14], [15], data analytics [16], etc.). Security and privacy are also an important concern when adding connectivity to cars [17]. However, the biggest challenge for any mobile communication technology is achieving the critical mass for the system to be economically viable. Regulatory issues (e.g., spectrum management, system interoperability, roaming...) may help to create the required ecosystem. Likewise, understanding deployment costs may help to quantify the initial investment [18], [19]. But, ultimately, it is system coverage that will determine system viability. Note that, unlike traditional telecommunication systems, which are first deployed in

The associate editor coordinating the review of this manuscript and approving it for publication was Meng-Lin Ku.

populated areas to maximize return of investment, connected car services require coverage to be provided first on roads and highways, even in remote areas of a country.

In that context, cellular vehicular communications (C-V2X) provide a faster time-to-market, compared with dedicated short-range V2V and V2I communications, which will take many years to reach the required penetration ratio of roadside and on-board units [20]. Current deployments based on legacy LTE networks (V2N2V and V2N2I) can offer basic C-ITS, which will be extended in the coming years with the new PC5 sidelink standardized in Release 14 (LTE-V2X) and improved latency and reliability of the New Radio Interface (5G-V2X).

In this work, a large drive test campaign in a commercial LTE network is presented. The aim is to characterize radio signal strength fluctuations on a medium scale (i.e., meters). For this purpose, radio signal level measurements are collected on a 1,000 km route covered by 2 vehicles. By comparing signal level samples at the same geographical location, taken at slightly different times, a statistical model of fluctuations is derived. Likewise, the impact of different factors on the signal level received from the serving cell is assessed. The rest of the paper is structured as follows. Section II revises related work. Section III outlines the experimental methodology. Section IV presents measurements taken with one of the cars (single-system analysis). Then, Section V shows the comparison of measurements from the two cars (dual-system analysis). Finally, Section VI presents the main conclusions of the work.

II. RELATED WORK

Propagation mechanisms in wireless networks have been thoroughly studied in the literature. The received signal is often modeled as the sum of three components, corresponding to macro-level signal attenuation (pathloss), primarily a function of distance to the base station, log-normal (a.k.a. slow) fading due to shadowing, with a correlation distance on the order of tens to hundreds of meters, and small-scale (a.k.a. fast) fading due to multipath, with a correlation distance on the order of less than a wavelength [21]. Several radio channel models have been proposed to explain rapid fluctuations, which are key in the design and performance evaluation of physical layer schemes [22], [23]. Likewise, slow fading effects are discussed in many papers (e.g., impact of environment [24], impact of terrain [25], spatial correlation between base stations [26], [27], angular correlation [28], etc.). These effects are important for network dimensioning, because the standard deviation of shadowing is used by operators to adjust link budget calculations in statistical coverage analysis [29]. If that parameter is set incorrectly, the number of required base stations to ensure the target coverage levels may be unnecessarily high (or excessively low). At the same time, correlated shadowing has a negative effect on the connectivity of wireless multi-hop networks (e.g., V2V networks) [30]. Neglecting shadowing correlation in vehicular networks could lead to unreliable system design and inaccurate simulation results.

In parallel, several field trials have shown the first benefits of C-V2X. For instance, in [31], the feasibility of teleoperated driving based on LTE networks is shown in a testbed. However, a more comprehensive analysis of drive test measurements shows that varying radio conditions and handovers could prevent achieving the required latency in certain spots and hours [32]. Even by switching between network operators, the feasibility ratio in LTE is only 80% [33]. In the latest LTE releases (e.g., LTE Advanced Pro), this problem can be partly solved by multiconnectivity [34]. More focused on 5G, a route-based coverage analysis methodology is proposed in [35] for ultra-dense cellular deployments with V2N communications at different carrier frequencies. It is shown that existing cellular networks, where small base stations are deployed at macro cell edge, traffic hotspots or coverage holes, may not be sufficient for V2N coverage at millimeter wave frequencies.

Closer to the work presented here, in [36], a nationwide drive test measurement campaign is presented to check if the original LTE requirements in terms of latency and handover performance are met, and to which extent 5G developments will reduce the existing gap. Moreover, a radio wave propagation tool tuned with road measurements is used to estimate coverage ratios for different terminals and environments with a low resolution grid (i.e., 50×50 meters). It shows that, for most safety and efficiency applications, road users can rely on basic LTE terminals, but indoor users (e.g., underground parking lots) might need specialized terminals (e.g., Narrowband Internet-of-Things, NB-IoT).

In this work, another nationwide drive test campaign in a commercial LTE network is presented. Unlike [36] and [37], the aim is not to assess general coverage and performance levels on roads, but to characterize radio signal strength fluctuations on a smaller scale (i.e., meters). By comparing signal level samples at the same geographical location, but at slightly different times, it is possible to characterize how different factors (e.g., shadowing, environment, handover ...) can impact the fluctuations of signal level received from the serving cell. Unlike many legacy studies on shadowing, which were developed in small urban scenarios, the analysis presented here is focused on road scenarios. Note that the different user speeds, line-of-sight conditions, obstacle sizes and radiating systems in roads might have a strong impact on propagation mechanisms. Likewise, prior studies are focused on propagation issues, neglecting the impact of radio resource management (e.g., handover). Results presented here can be used by cellular operators to derive the required safety margins in link budget calculations specifically for road traffic. Likewise, results can be used to derive more accurate shadowing models for C-V2X vehicular networks. Moreover, the selected methodology can easily be replicated, since it adopts the measurement setup used for benchmarking cellular operators around the world. Thus, network operators can reuse signal level measurements collected

for other purposes to repeat and extend the analysis presented here.

III. EXPERIMENTAL METHODOLOGY

This section outlines the measurement process, the pre-processing of data to reduce location errors and the data analysis methodology.

A. MEASUREMENT SET-UP

The measurement campaign was conducted in a northern country of the European Union. It adopts the de-facto standard used in more than 80 countries for benchmarking cellular operators [38]. The geographical area under analysis covers the major roads of the country, including highways and urban roads. To this end, two cars covering the same route collected radio signal level measurements from the serving cell while making voice calls and downloading data. Both cars (hereafter referred to as car 1 and 2) move independently, and the distance between them (measured in time) may fluctuate from 10 seconds to 60 minutes. Car speeds varied from 0 to 170 km/h. Measurements were made from 8 a.m. to 18 p.m. Monday to Saturday during 3 weeks in March 2020, for a total of 1,000 km.

Each car was equipped with 2 Samsung Galaxy S10 terminals, one for making voice calls and another for sending/receiving packet data. Both of them were located inside a box in the rear window of the car. Terminals worked independently (i.e., not synchronized). In this work, the analysis is only focused on the reference signal received power (RSRP) from the LTE cell serving the terminals dealing with packet data. The coverage analysis is restricted to LTE 1800 + band (earfcn 1617, 1846.7 MHz downlink, 20 MHz system bandwidth). At the same time, location was recorded per measurement sample via GPS and later used to generate averages of the received signal power every half a second. Both RSRP and GPS measurements were directly taken from the S10 terminals. The resulting dataset contains 614,444 and 679,232 samples for car 1 and car 2, respectively. Later, latitude and longitude were rounded to the fourth decimal place, leading to a spatial resolution of 6-7 meters (i.e., 7×7 meter tile).

Measurements are tagged to allow separate analysis of open roads, towns and cities. Following the same names in [38], the term 'road' is used here to denote open roads, and 'towns' and 'cities' to denote streets and roads in those urban environments. Note that, as there are more locations on open roads than on urban environments, overall figures tend to reflect the situation of the former unless the analysis is segregated per environment.

B. TRACE CONSTRUCTION

To visualize data on a map, the mobility trace of each car is constructed, showing car position with time in a bidimensional grid. Time resolution is 0.5 seconds. Thus, depending on car speed, the distance between consecutive locations ranges from 0 (e.g., when car is stopped) to several tiles away

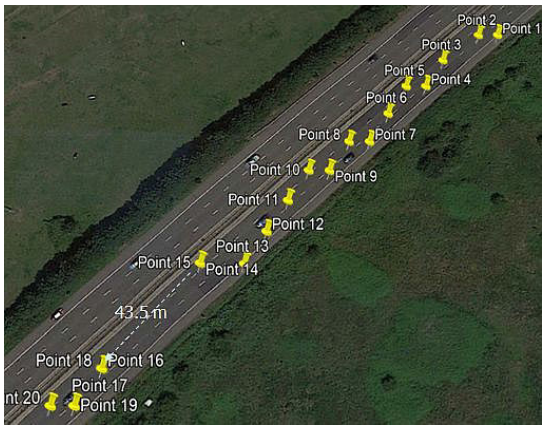

(a) GPS loss.

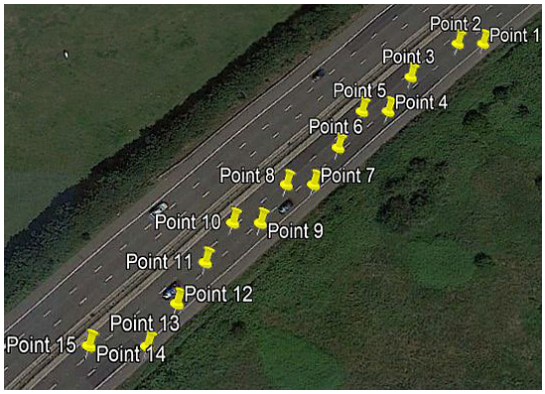

(b) GPS uncertainty.

FIGURE 1. An example of mobility trace.

(e.g., in the highway). For ease of comparison, both cars share the same time reference.

A preliminary analysis of traces shows the existence of location errors due to temporary loss of GPS signal, even in open roads. Fig. 1(a) shows an example of mobility trace with a GPS loss event. In the measurement system, when GPS is lost, the previous location is maintained until the GPS signal is recovered. Such a behavior causes that several consecutive reports are located in a wrong position. These errors can easily be detected (and eliminated) by processing mobility traces. In the figure, the GPS loss results in a jerky movement, observed as several samples located at the same position followed by a sudden jump to a distant location (43.5 m in this example). These events can be detected by estimating the instantaneous speed of the car (in meters/s) from consecutive location measurements as

$$v[n] = \frac{\sqrt{(x[n] - x[n-1])^2 + (y[n] - y[n-1])^2}}{t[n] - t[n-1]}, \quad (1)$$

where n denotes sample index, v is car speed, x and y are Cartesian coordinates (Easting and Northing) computed by WGS84 map projection (in meters), and t is the time when measurement was taken (in seconds). In most cases, $t[n] - t[n-1] = 0.5$ s. In this work, all samples with

estimated car speed above 50 m/s (180 km/h) are tagged as GPS losses. Once detected, the effect of GPS losses could be circumvented by taking only the first measurement per location. In this work, for reliability, all samples with zero car speed immediately before and after a GPS loss event are also discarded, since any GPS loss points out a weak GPS signal. These discarded samples are only 3% of measurements.

A visual inspection of traces also shows the presence of small positioning errors due to GPS noise (GPS uncertainty). Fig. 1(b) shows the same trace as Fig. 1(a), but enlarged. It is observed that the car's trajectory is not a straight line, but a curve. Deeper analysis reveals a regular movement pattern (i.e., first left, then down/diagonal) that depends on road orientation and whose repetition period varies slightly in time. Such a fixed pattern (and the fact that the estimated car position always falls on the road) suggests that GPS uncertainty is small and most of the error comes from the rounding operation introduced by tile resolution.

Mobility traces have also been used to interpret the results. Many of the findings presented next have been revealed by mapping the traces.

C. DATA ANALYSIS METHODOLOGY

The aim of the analysis is to characterize fluctuation of radio signal strength observed at the same location. To this end, signal measurements taken at the same tile of the map at different times are compared. The ultimate goal is to provide a statistical model for these fluctuations and understand the underlying mechanisms. In theory, signal level differences might be due to:

a) measurement system differences (e.g., terminal, car, in-car position),
b) positioning errors (e.g., GPS loss, GPS uncertainty),
c) changes in far environment (e.g., weather, wind, temperature gradients),
d) changes in near environment (e.g., shadowing or reflection by nearby objects),
e) multipath fading (e.g., relative phase/strength of reflections), or
f) radio resource management (e.g., handover to a different serving cell).

To isolate the above sources of deviation, the analysis is broken down in two stages. First, the analysis is focused on measurements of a single car (single-system analysis). Then, the analysis is extended to measurements from both cars at the same location (dual-system analysis).

IV. SINGLE-SYSTEM ANALYSIS

The analysis is first focused on the trace of car 1. The aim is to check the behavior of fluctuations when the car is moving and when the car is stopped.

A. CORRELATION DISTANCE

The analysis starts by checking the correlation distance of radio signal levels. In simple terms, correlation distance

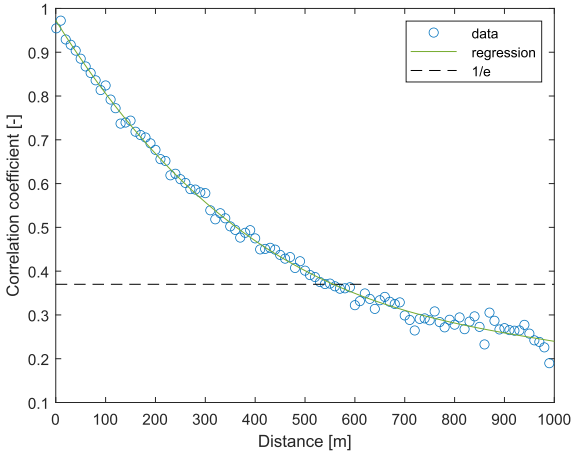

(a) All environments.

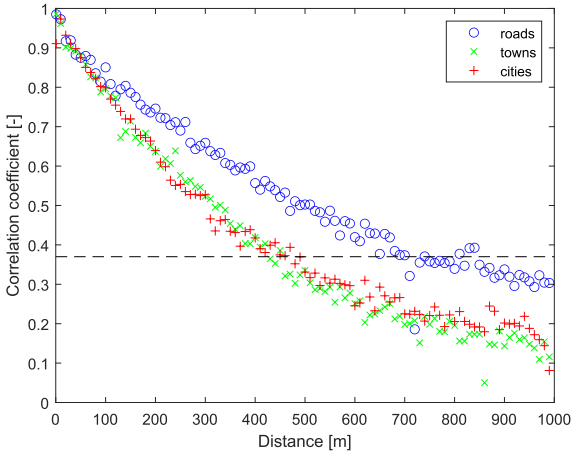

(b) Per environment.

FIGURE 2. Distance autocorrelation function.

reflects the distance a car must travel from an original location to receive a power level from the serving cell significantly different. For this purpose, the distance autocorrelation function, $R(x)$, is derived by computing the correlation coefficient between a pair of signals, $s_d[n]$ and $s_{d+x}[n]$, representing the signal level of points separated x meters apart. The samples of each of these signals are defined by repeatedly selecting a reference point in the trace for $s_d[n]$ and finding the next point in the trace at x meters (if exists) for $s_{d+x}[n]$. Then, the correlation distance is defined as the distance where autocorrelation falls below $1/e = 0.37$ [24].

Fig. 2(a) shows the distance autocorrelation function when the whole trace of car 1 is considered. It is observed that the correlation distance is around 555 meters. Likewise, Fig. 2(b) shows the distance autocorrelation function of car 1 segregated by environment. As expected, the correlation distance in roads (710 m) is larger than in towns and cities (430 m).

B. SIGNAL LEVEL FLUCTUATIONS IN A LOCATION

Even if signal level is nearly the same in locations within the correlation distance (when compared to the full range of

possible RSRP values, from −140 dBm to −44 dBm), small differences still exist. A closer look at Fig. 2(a) reveals that the correlation coefficient is not 1 as distance approaches to zero. On the contrary, autocorrelation is only 0.95 when distance is zero. This observation points to the existence of fluctuations in the signal level received at the same tile (i.e., the signal level received at the same tile varies with time).

To characterize those deviations, it is exploited that the car is sometimes stationary, so that several consecutive samples are taken at the same tile. A comprehensive analysis of traces shows that the duration of static periods ranges from a few seconds (e.g., road cross, traffic jam, traffic light…) to minutes (e.g., driver change, coffee break…) and up to half an hour (e.g., lunch). Static periods can be identified in traces by checking that the distance traveled between consecutive samples is zero (provided that GPS losses have been eliminated). Period duration is calculated by counting the number of samples where location is maintained. Then, the fluctuation term can be isolated by subtracting the average signal level of the period. By concatenating all periods, a single signal with all the fluctuations is constructed (referred to as fluctuation signal). To increase the robustness of the analysis, only static periods of more than 5 seconds (i.e., 10 samples) are considered. This constraint is fulfilled by 2,417 periods in car 1, with a total of 169,203 measurement samples.

Fig. 3(a) and 3(b) present the histogram and cumulative density function (CDF) of the fluctuation signal with all static periods in car 1, segregated per environment. In Fig. 3(a), it is observed that most samples show a deviation from the average smaller than 2 dB. From Fig. 3(b), it is inferred that 90% of measurements are less than 2.2 dB from average (1.8 dB for roads, 2.4 dB for cities).

TABLE 1. Statistics of signal fluctuation in static periods [dB].

Statistic/Environment	All	Roads	Towns	Cities
Average	2.0 e-5	1.0 e-2	1.5 e-2	-6.0 e-5
Standard deviation	2.042	1.317	1.362	2.501
Median	0.024	0.058	0.023	0.015
Skewness	1.41	-1.10	-0.35	1.54
Kurtosis	42.6	16.33	11.25	35.32

Table 1 presents the main statistics of the fluctuation signal. For clarity, the most interesting findings are highlighted in gray. First, the large kurtosis value points out that most deviation samples are concentrated around the center of the distribution (0 dB). Second, the larger standard deviation in cities confirms that fluctuations in static periods are larger in urban scenarios. Finally, the negative skewness value in roads indicates that the distribution is slightly shifted to the right (i.e., positive signal level deviations prevail). This might be due to the fact that, in roads, most locations have line-of-sight conditions to the serving base stations. The opposite is true for cities, where more locations have non-line-of-sight conditions to the serving base station.

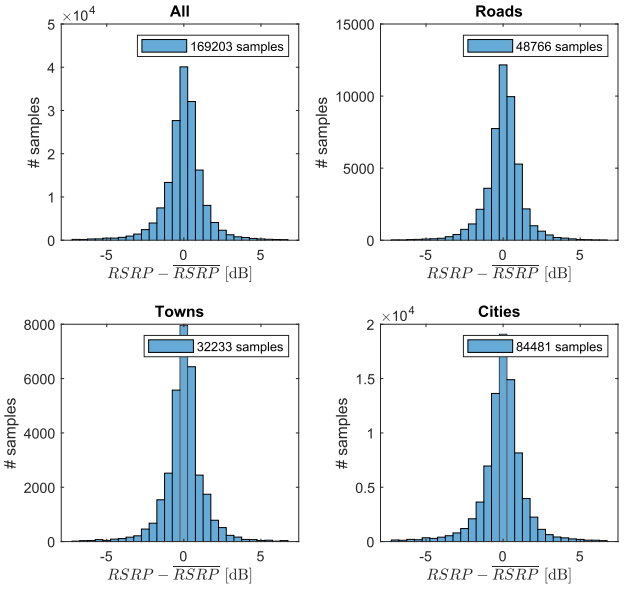

(a) Histogram.

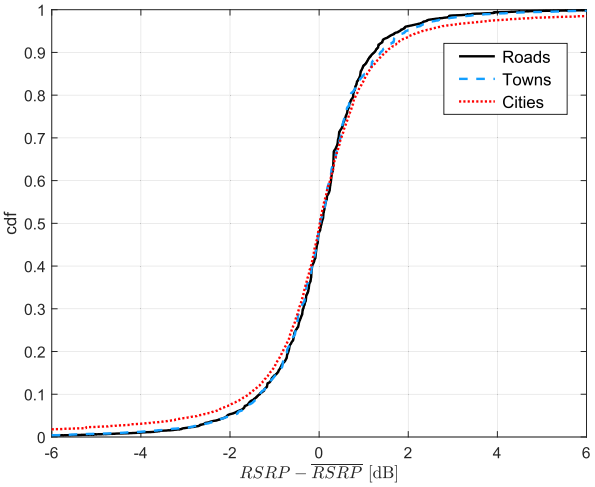

(b) Cumulative density function.

FIGURE 3. Distribution of signal fluctuations in static periods.

Likewise, the fluctuation speed is evaluated by computing the zero crossing frequency[1] per period in the fluctuation signal. Fig. 4 shows the CDF of the zero crossing rate per period in different environments. It is observed that the median zero crossing rate is around 0.2 Hz in all of them, even if rates are slightly higher in cities.

It should be pointed out that the above definition of static period not only considers periods when the car is fully stopped, but also when the car is slowly moving. Note that, in the latter case, 10 consecutive samples are reported at the same tile as long as the car's speed is less than (7 m)/(5 s) = 1.4 m/s. To check if car movement makes any difference, a differentiated analysis has been carried out by segregating static periods above and below 1 m/s. Results (not presented

[1]The zero crossing frequency (or rate) of a signal is the number of times the signal changes sign in a given period of time (usually one second).

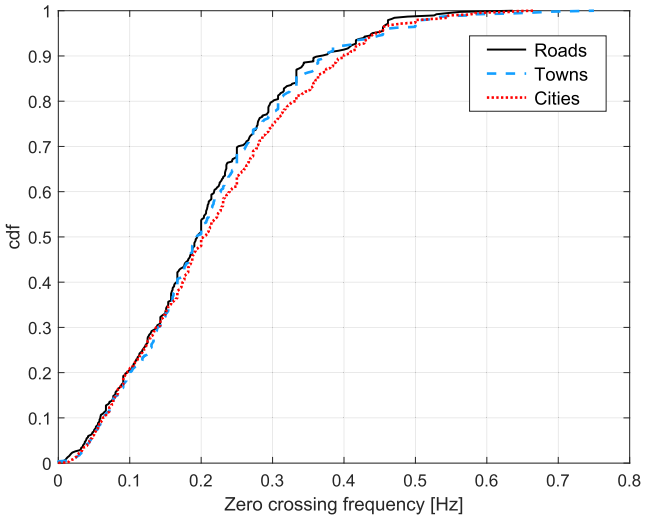

FIGURE 4. Distribution of zero crossing frequency per period.

here) show that fluctuations are exactly the same for fully static and slowly moving periods in all environments.

C. STATISTICAL MODEL OF FLUCTUATIONS IN STATIC PERIODS

An analytical model is derived from measurements by fitting a classical probability distribution by the maximum likelihood (ML) method. The large kurtosis values observed in Table 1 suggest that data has a heavy-tailed distribution. Based on this observation, a preliminary set of candidate distribution models is selected. The final distribution is chosen by checking the probability plot of distributions and selecting that with the minimum deviation in extreme probability values. Thus, a t-location-scale distribution is selected, whose probability density function is given by

$$f(x|\mu,\sigma,\alpha) = \frac{\Gamma(\frac{\alpha+1}{2})}{\sigma\sqrt{\alpha\pi}\,\Gamma(\frac{\alpha}{2})}\left[\frac{\alpha+(\frac{x-\mu}{\sigma})^2}{\alpha}\right]^{-(\frac{\alpha+1}{2})}, \quad (2)$$

where $\Gamma(*)$ is the gamma function, μ is the location parameter, σ is the scale parameter and α is the shape parameter. Table 2 shows the ML estimates of the three parameters of the distribution for different environments, together with their 95% confidence intervals.

For instance, Fig. 5 shows the probability plot comparing the percentiles of static measurements against those of the fitted normal and t-location-scale distributions in road environments. Numbers in the legend denote parameter estimates (i.e., mean/standard deviation in normal distribution and location/scale/shape in t-location-scale distribution). It is observed that the normal distribution fails to reflect the tails of the distribution. In contrast, the t-location-scale distribution better approximates the low percentiles of the data distribution (i.e., signal drops much lower than the average). Yet, a quantitative analysis (not presented here) shows that the t-location-scale distribution does not pass the chi-square goodness-of-fit test [39]. Similar results are observed in towns and cities (not presented for brevity).

TABLE 2. Parameters of t-location-scale distribution for fluctuations in static periods.

Environment	Parameter	Estimated value	Confidence interval
Roads	μ	0.0575	[0.0497, 0.0654]
	σ	0.706	[0.697, 0.714]
	α	2.413	[2.349, 2.479]
Towns	μ	0.0379	[0.0278, 0.0479]
	σ	0.732	[0.721, 0.744]
	α	2.374	[2.298, 2.453]
Cities	μ	0.0312	[0.0247, 0.0378]
	σ	0.725	[0.718, 0.732]
	α	1.569	[1.546, 1.592]

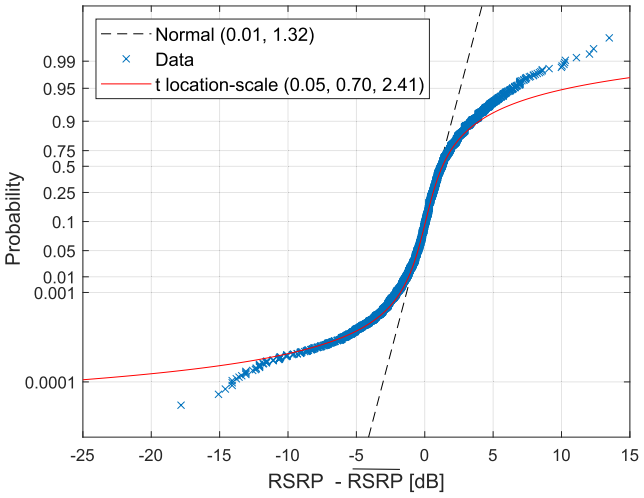

FIGURE 5. Probability plot of distributions for signal fluctuations of static periods in road environments.

D. ORIGIN OF FLUCTUATIONS IN STATIC PERIODS

In Table 1, it has been shown that signal level fluctuates more than 2.2 dB for static periods, but these fluctuations are 33% larger (and slightly faster) in cities than in roads. Likewise, fluctuations are the same for static and slow moving users. Based on these results, the potential sources of fluctuation in static periods are assessed, leading to the hypotheses presented in Table 3.

The use of a single system ensures that deviations are not due to differences in the measurement system. Positioning errors are neither the main cause of fluctuations, since GPS losses are eliminated by data pre-processing and GPS uncertainty (plus rounding) is reduced by the time constraint introduced to define static periods, where samples must be consecutive (i.e., measurements reported at the same location due to a location error, but taking place after the end of the period, are discarded). Likewise, should the far environment be the source of fluctuations, these would be larger in open roads, where distance to the base station is larger. Similarly, if multipath fading exists (because tile size was not large enough to remove its effect), fluctuations at the same tile

TABLE 3. Reasons for signal level fluctuations in static periods.

Reason	Impact
Measurement system differences (e.g., terminal, car, in-car position)	No
Positioning errors (GPS losses, GPS uncertainty)	No
Changes in far environment (e.g., weather, wind, temperature gradients)	Unlikely
Changes in near environment (e.g., shadowing or reflection by nearby objects)	Yes
Multipath fading (e.g., relative phase/strength of reflections)	No
Radio resource management (e.g., handover to different serving cell)	Unlikely

would have to be larger for slowly moving users than for static users. Recall that tile resolution is 7 meters (i.e., 43 times the wavelength at 1847 MHz). Finally, it is very unlikely that a static user changes serving cell. For all these reasons, it is expected that signal fluctuations for static users are mainly due to changes in the near environment (e.g., temporal shadowing by a pedestrian or another vehicle).

V. DUAL-SYSTEM ANALYSIS

The following paragraphs describe the comparison of measurements from the two cars. Hereafter, system 1 denotes the Samsung Galaxy S10 handset in car 1 and system 2 denotes the Samsung Galaxy S10 handset in car 2.

The aim is to check signal differences when cars are at the same tile. For this purpose, tiles crossed by the two cars are identified from traces. Note that, even if both cars follow similar routes, small path differences may still exist (e.g., different lane in the highway). Likewise, sampling at 2 Hz (i.e., period of 0.5 s) causes that car trajectory on the map is discontinuous when the car is traveling at high speeds. As shown in Fig. 1, points consecutive in the trace may be 3-4 tiles apart on the map in highways. Likewise, positioning errors due to GPS uncertainty and rounding may occasionally move the point to the adjacent tile. All these factors make that only a small set of points in both traces share exactly the same location. Specifically, 96,443 common samples (out of 593,858 in car 1 and 661,521 in car 2) are found after pre-processing (i.e., approximately 15%). Nonetheless, the dataset is large enough to provide significant results.

In each tile, signal level, instantaneous car speed and time lapse between measurements are computed. To discard any difference between the measurement systems installed on the two cars, Fig. 6 shows a scatter plot of the signal level received by the cars at the same tile. It is observed that RSRP measurements are strongly correlated between systems, evident from the high value of the sample determination coefficient ($R^2 = 0.89$). Likewise, the slope of the regression curve is nearly 1, without any significant bias on the range of interest. Nonetheless, significant deviations are observed in some tiles (highlighted by arrows).

To break down these deviations, Fig. 7 (a)-(b) show the histogram and CDF of their distribution. For comparison purposes, in Fig. 7(b), the CDF of fluctuations for static users is also superimposed. At first sight, it is clear that deviations between the 2 cars are much larger than fluctuations for static

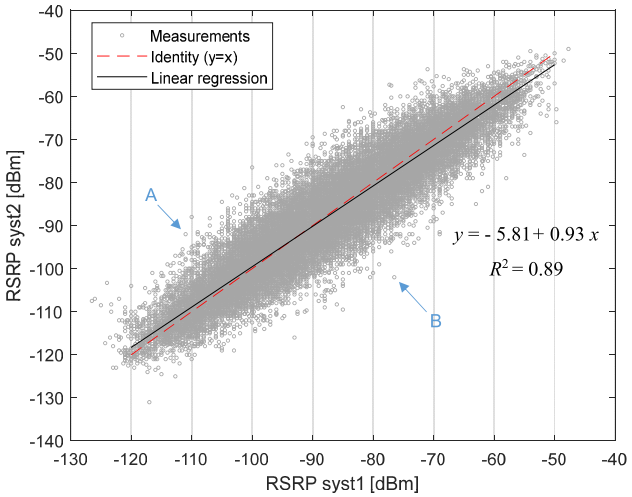

FIGURE 6. Correlation between measurements from cars at the same location.

users. Specifically, the 5th and 95th percentiles of the distribution of signal differences between systems are -6.5 and 6.2 dB, respectively, compared to -2.3 and 2.1 dB for fluctuations in static users (i.e., 4 dB larger). Closer analysis (not presented here) confirms that the magnitude of fluctuations does not depend on the time lapse between the measurements of both systems (neither when time difference is in the order of seconds nor hours).

Fig. 8 shows the CDF of signal level differences between systems per environment. It is observed that larger positive deviations exist on roads, whereas larger negative deviations occur in cities. This result is just a consequence of the different skewness factors, already observed when analyzing the measurements of car 1 in Table 1.

A. STATISTICAL MODEL OF DIFFERENCES BETWEEN CARS

As for static users, an analytical model is derived for signal level differences between cars by fitting a probability distribution selected a priori. In this case, a logistic distribution is chosen, whose probability density function is given by

$$f(x|\mu,\sigma) = \frac{e^{-\frac{x-\mu}{\sigma}}}{\sigma\,(1+e^{-\frac{x-\mu}{\sigma}})^2}\ , \tag{3}$$

where μ is the location parameter and σ is the scale parameter. Table 4 shows the ML estimates of the logistic parameters in the different environments.

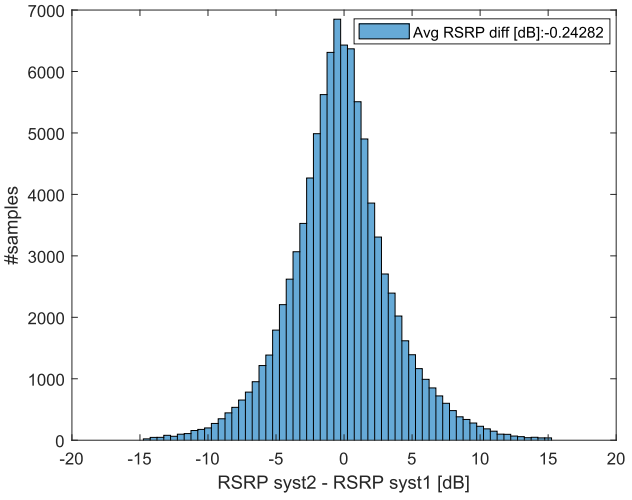

(a) Histogram.

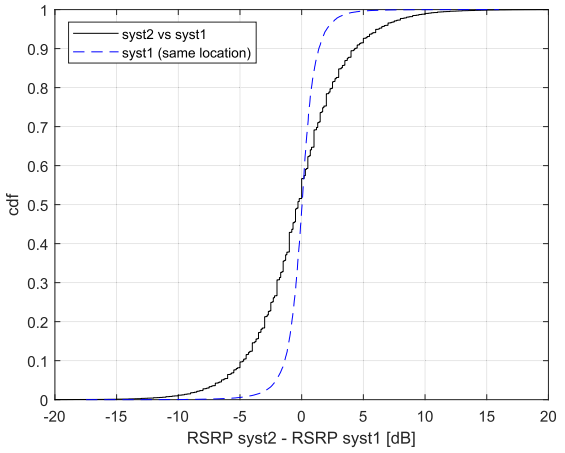

(b) Cumulative density function.

FIGURE 7. Distribution of signal level differences between co-located systems.

TABLE 4. Parameters of logistic distribution for differences between co-located systems per environment.

Environment	Parameter	Estimated value	Confidence interval
Roads	μ	0.0575	[0.0497, 0.0654]
	σ	0.706	[0.697, 0.714]
Towns	μ	0.0379	[0.0278, 0.0479]
	σ	0.732	[0.721, 0.744]
Cities	μ	0.0312	[0.0247, 0.0378]
	σ	0.725	[0.718, 0.732]

Fig. 9 shows the probability plot with percentiles of measurements and fitted distributions for signal differences between cars in road environments. As for fluctuations in static users, the normal distribution fails to reflect the tails of the distribution of signal differences between cars at the same location. In contrast, the logistic distribution closely approximates the data distribution for extreme percentiles, even if it neither passes the chi-square goodness-of-fit test. Again, the same trends are observed in towns and cities (not presented for brevity).

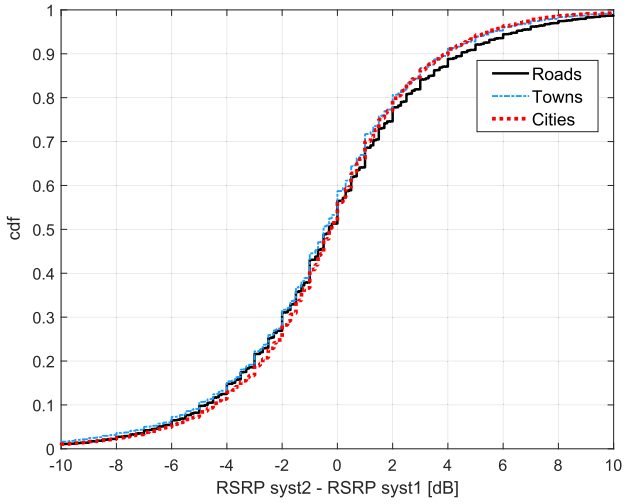

FIGURE 8. Signal level differences between co-located systems per environment.

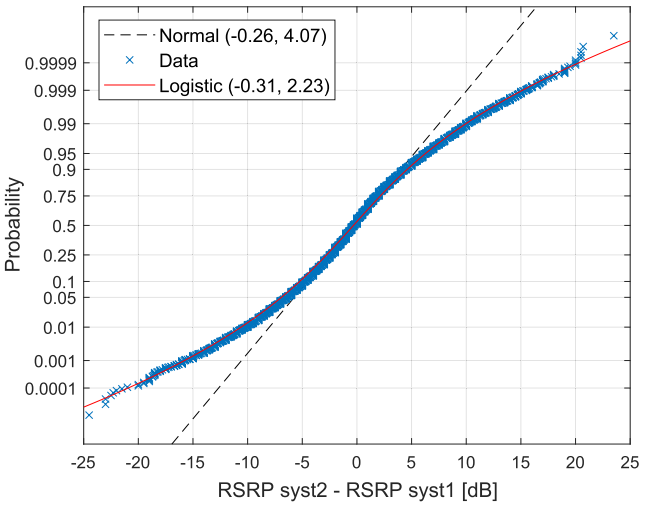

FIGURE 9. Probability plot of distributions for signal deviations between co-located systems in road environments.

B. ORIGIN OF DIFFERENCES BETWEEN CARS

To unveil the origin of extreme deviations, a more detailed analysis of outliers is carried out. In particular, the analysis is focused on the 2 points highlighted in Fig. 6, showing very large positive and negative differences between cars.

The outlier A on the upper-left of the figure has −111 dBm for system 1 and −92 dBm for system 2 (19 dB deviation). Fig. 10 (a)-(c) present a detailed analysis of the trace, signal level and speed of both cars around the event. For ease of analysis, in the photo in Fig. 10(a), the trace followed by each of the car is depicted in a different color, highlighting common points. Likewise, signal level and speed in Fig. 10(b) and 10(c) are not presented against time, but location (latitude), since both cars can move at different speeds, as deduced from Fig. 10(c). Note that the time axis goes from right to left, as cars are heading south (i.e., decreasing latitude). In Fig. 10(a), it is observed that both trajectories coincide in many points. A closer inspection of

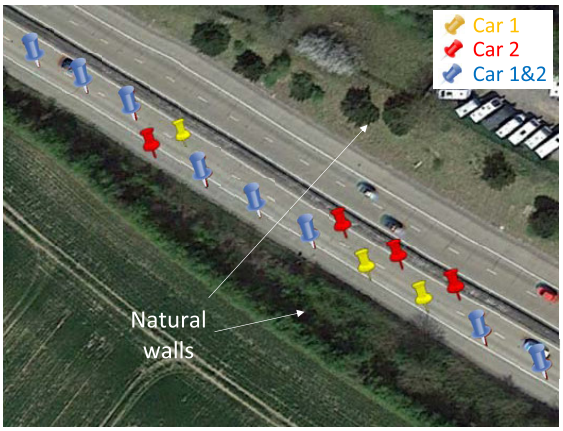

(a) Trace.

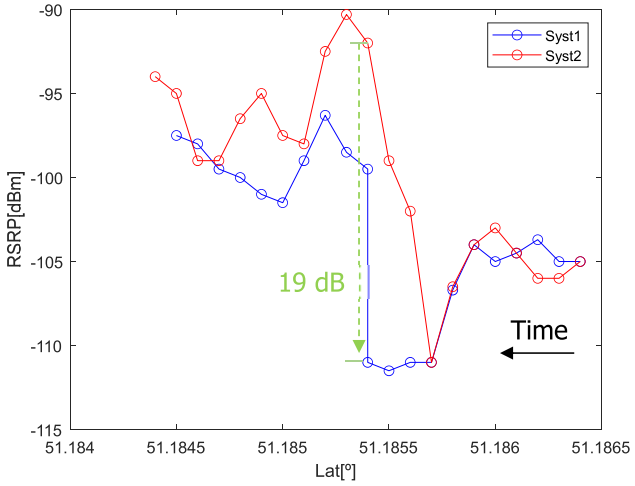

(b) Signal level.

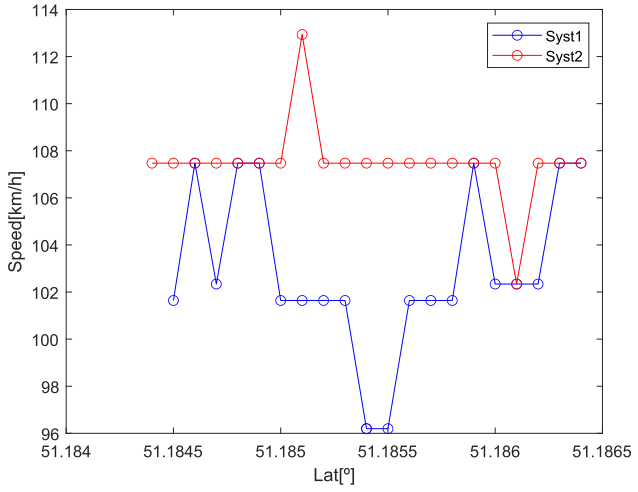

(c) Car speed.

FIGURE 10. Analysis of outlier 1 (natural wall corridor).

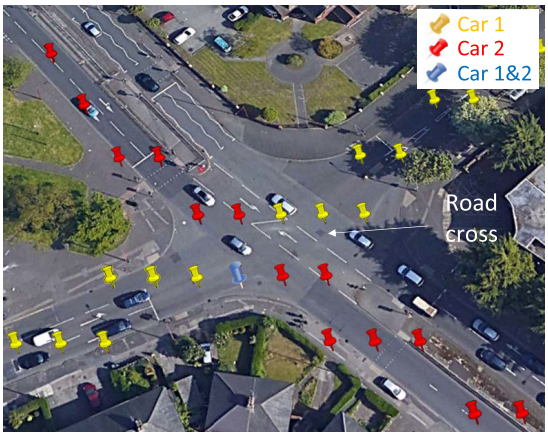

(a) Trace.

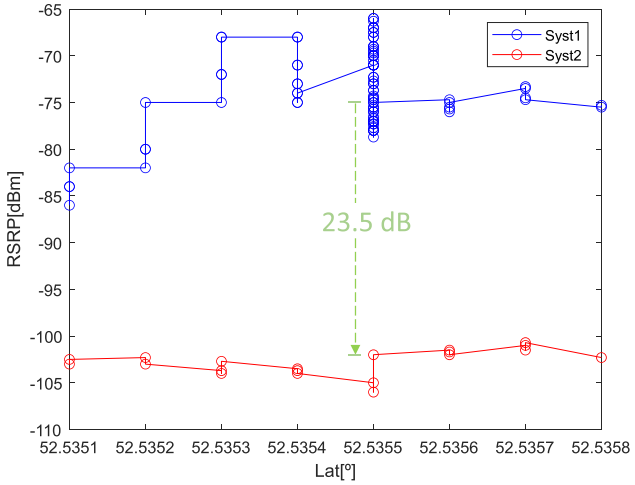

(b) Signal level.

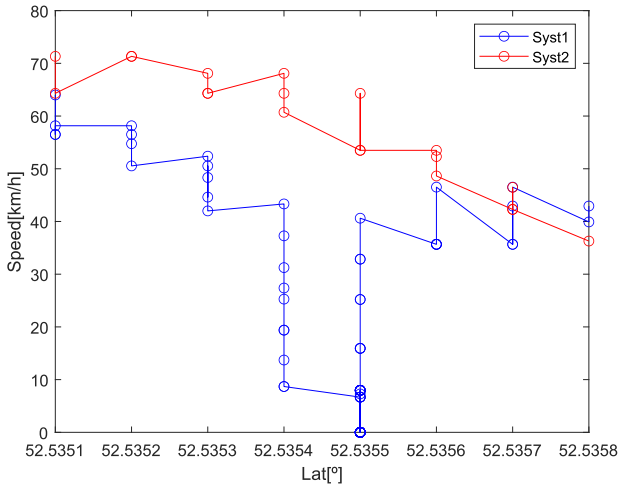

(c) Car speed.

FIGURE 11. Analysis of outlier 2 (road cross).

the orthophoto shows that the analyzed road segment is surrounded by natural walls, which causes an obstruction of the line of sight to the serving base station. Such an event is also evident in Fig. 10(b), where it is observed that signal level decreases from −105 to −110 dBm at the beginning of the trace (right) in both systems. From that point, both systems differ. System 1 experienced a large increase of signal level, while system 2 experiences a similar increase but 3 samples

TABLE 5. Reasons for signal level differences between co-located systems.

Reason	Impact
Measurement system differences (e.g., terminal, car, in-car position)	No
Positioning errors (GPS losses, GPS uncertainty)	Yes (normal)
Changes in far environment (e.g., weather, wind, temperature gradients)	Unlikely
Changes in near environment (e.g., shadowing or reflection by nearby objects)	Yes
Multipath fading (e.g., relative phase/strength of reflections)	No
Radio resource management (e.g., handover to different serving cell)	Yes (extreme)

(1.5 s) later. Thereafter, both systems follow a similar trend. A careful inspection of traces shows that the abrupt change in signal level is due to a change of serving cell (i.e., handover). In case of system 1, the handover to the new (stronger) cell is delayed a few seconds for some reason (e.g., new base station temporarily shadowed by another vehicle).

A similar phenomenon is observed in the outlier B at lower-right of the curve in Fig. 6. In this case, system 1 displays −76.5 dBm and system 2 −102 dBm (23.5 dB deviation). Fig. 11 (a)-(c) again show the trace, signal level and car speed associated to the event. The orthophoto in Fig. 11(a) shows a road cross surrounded by houses in a suburban area of a city. Note that, in this case, the 2 cars follow completely different routes, intersecting in a single common location. From Fig. 11(c), it is inferred that car 1 stops at the cross (as speed becomes zero), while car 2 does not stop. More importantly, it is observed that none of the systems changes signal level as they go through the cross, even if the signal received by system 1 at the common location is many decibels above that of system 2. Such a difference comes from a different serving cell. It is hypothesized that system 2 does not trigger a handover to the cell serving system 1 because it traverses the cross at more than 50 km/h.

Based on the above observations, Table 5 summarizes the hypotheses on the origin of deviations for moving users. The reasons for the larger differences compared to static users are highlighted in gray. Deviations are not due to measurement systems, because both use the same handset model and are located at the same position in the car (rear window). However, location errors are larger than for static users, as no time constraint is considered when selecting the pair of measurements to be compared. It was shown in Fig. 1(b) that GPS uncertainty and latitude/longitude rounding may take a measurement to the adjacent tile, 7 meters away. In the vicinity of small obstacles (e.g., vehicle, tree, signboard…), such a small distance is the difference between being in line of sight or not to the base station. Therefore, it is expected that positioning errors are the main reason behind the 4 dB larger 95^{th} tile compared to fluctuations of static users. Moreover, the outlier analysis has shown that extreme deviations are normally due to handover procedures, causing that the two systems, traveling at different speeds (and sometimes in different directions), are not served by the same cell. Such a handover behavior is influenced by network settings (e.g., hysteresis and timers), operator policy (e.g., default carrier for certain services) or network hierarchy (e.g., target base station assigned to a different core network element).

VI. CONCLUSION

Understanding the fluctuations of the radio signal received by mobile users at a certain location is key for setting the right safety margins in cellular network planning. Such a piece of information will be important in road scenarios for applications that require ultra-reliable low-latency communications. In this work, a comprehensive analysis of radio signal strength fluctuations on roads in a LTE system has been presented. The analysis is based on a nationwide drive test with 2 cars sharing the same measurement system.

The analysis of measurements from one of the cars has shown that correlation distance is 710 m in open roads and 430 m in towns and cities. These values can be used to define the spatial grid resolution in radio network planning tools for road coverage scenarios. Defining tile size above correlation distance is a waste of computational resources, whereas defining it below might cause that coverage issues are not detected due to lack of spatial detail. Moreover, the analysis of static periods has shown fluctuations around 1.8 and 2.2 dB in roads and cities, respectively. These deviations are mostly due to changes in shadowing conditions caused by other vehicles.

The comparison of measurements between cars has shown typical deviations of more than 6 dB in all road scenarios. Even if part of these deviations are due to positioning errors in the measurement system, these highlight an important issue, which is the fact that adjacent tiles separated only a few meters may have different coverage levels. Thus, different lanes on the road would receive different signal levels from the serving cell (typical lane width is around 3.5 m). Also important, extreme deviations of more than 23 dB have been observed at the same location caused by differences in the serving cell due to handover procedures. It is expected that deviations will be even larger for real users, since they have different handset models, vehicle class and pathloss environment inside vehicle (e.g., pocket, glovebox…).

The risk of neglecting those extreme signal fluctuations is underestimating propagation losses. This action would lead to an optimistic maximum cell radius in network dimensioning and overconfident performance predictions in radio network planning for services requiring high reliability in roads. Ultimately, both effects might degrade the performance of ultra-reliable low-latency services needed for connected car applications in live 5G systems. This problem can be avoided by increasing safety margins in the link budget of these services. It should be pointed out that, even if all these deviations negatively affect network costs as more base stations are

needed, they add diversity to C-V2N communications, which can be exploited by the multiconnectivity feature in 5G to achieve more reliable links.

Future work will repeat the tests with different handsets (4G-only vs 5G-capable), services (voice vs data), bands (800/1800/2100/2600 MHz, 3.5/26 GHz) and radio access technologies (4G vs 5G). These tests will check to which extent the results presented here can be generalized. It is envisaged that the influence of the specific measurement setup (e.g., terminal, in-car position, etc.) should be small, provided that the same setup is maintained in the two cars. Even if this was not the case, the values derived for model parameters correspond to a typical situation. Nonetheless, it would be interesting to characterize deviations due to in-car losses (different cars or different positions inside car) and synchronization issues when handsets are at the same car. In 5G systems, it would be expected that similar results are obtained, provided that the same frequency is used. However, preliminary tests have shown that terminal and service diversity causes extreme signal deviations at the same location (> 50 dB) due to the traffic management policy of the operator. For example, a user at the same location might be served by different carriers depending on the requested service. Likewise, certain handsets might be pushed to or kept in different frequency bands / technology layers. Such occurrences are associated with the rollout of a new radio technology and are likely to disappear once it is deployed widely across the network. Also, in the millimeter band, severe weather conditions (e.g., rain or fog) and higher penetration losses (due to, e.g., metalized car windows) will increase the magnitude of fluctuations.

REFERENCES

[1] R. El Hattachi and J. Erfanian, "5G white paper," NGMN, Frankfurt, Germany, White Paper version 1.0, Feb. 2015.
[2] Y. Gao and A. Wachtel, "Connecting cars on the road to 5G," Huawei, Shenzhen, China, White Paper, 2017.
[3] Accessed: Jul. 23, 2020. [Online]. Available: https://www.alliedmarketresearch.com/connected-car-market
[4] C. Boberg, M. Svensson, and B. Kovacs, "Distributed cloud, automotive and industry 4.0," *Ericsson Technol. Rev.*, no. 11, pp. 1–12, Nov. 2018.
[5] *Study LTE-Based V2X Services (Release 14)*, Standard TR 36.885, V14.0.0, 3GPP, Jun. 2015.
[6] *Study on Architecture Enhancements for the Evolved Packet System (EPS) and the 5G System (5GS) to Support Advanced V2X Services*, Standard TR 23.786, V16.1.0, 3GPP, Jun. 2019.
[7] T. Lohmar, A. Zaidi, H. Olofsson, and C. Boberg, "Tranforming transportation with 5G," *Ericsson Technol. Rev.*, no. 13, Sep. 2019.
[8] A. Kwoczek *et al.*, "5G automotive vision," 5G-PPP, White Paper, 2015.
[9] F. J. Martin-Vega, M. C. Aguayo-Torres, G. Gomez, J. T. Entrambasaguas, and T. Q. Duong, "Key technologies, modeling approaches, and challenges for millimeter-wave vehicular communications," *IEEE Commun. Mag.*, vol. 56, no. 10, pp. 28–35, Oct. 2018.
[10] C. Chen, B. Wang, and R. Zhang, "Interference hypergraph-based resource allocation (IHG-RA) for NOMA-integrated V2X networks," *IEEE Internet Things J.*, vol. 6, no. 1, pp. 161–170, Feb. 2019.
[11] W. Xu, H. Zhou, H. Wu, F. Lyu, N. Cheng, and X. Shen, "Intelligent link adaptation in 802.11 vehicular networks: Challenges and solutions," *IEEE Commun. Standards Mag.*, vol. 3, no. 1, pp. 12–18, Mar. 2019.
[12] X. Li, L. Ma, Y. Xu, and R. Shankaran, "Resource allocation for D2D-based V2X communication with imperfect CSI," *IEEE Internet Things J.*, vol. 7, no. 4, pp. 3545–3558, Apr. 2020.
[13] J. Mei, X. Wang, and K. Zheng, "Intelligent network slicing for V2X services toward 5G," *IEEE Netw.*, vol. 33, no. 6, pp. 196–204, Nov. 2019.
[14] F. Giust, V. Sciancalepore, D. Sabella, M. C. Filippou, S. Mangiante, W. Featherstone, and D. Munaretto, "Multi-access edge computing: The driver behind the wheel of 5G-connected cars," *IEEE Commun. Standards Mag.*, vol. 2, no. 3, pp. 66–73, Sep. 2018.
[15] J. Zhang and K. B. Letaief, "Mobile edge intelligence and computing for the Internet of vehicles," *Proc. IEEE*, vol. 108, no. 2, pp. 246–261, Feb. 2020.
[16] H. Zhou, W. Xu, J. Chen, and W. Wang, "Evolutionary V2X technologies toward the Internet of vehicles: Challenges and opportunities," *Proc. IEEE*, vol. 108, no. 2, pp. 308–323, Feb. 2020.
[17] K. Strandberg, T. Olovsson, and E. Jonsson, "Securing the connected car: A security-enhancement methodology," *IEEE Veh. Technol. Mag.*, vol. 13, no. 1, pp. 56–65, Mar. 2018.
[18] M. Fallgren and K. Manolakis, Eds., "A study on 5G V2X deployment," 5G-PPP, White Paper Version 1.0, Feb. 2018.
[19] "C-ITS vehicle to infrastructure services: How C-V2X technology completely changes the cost equation for road operators," 5GAA, White Paper, Jan. 2019.
[20] Y. Yang and K. Hua, "Emerging technologies for 5G-enabled vehicular networks," *IEEE Access*, vol. 7, pp. 181117–181141, Dec. 2019.
[21] T. Rappaport, *Wireless Communications: Principles and Practice*, 2nd ed. Upper Saddle River, NJ, USA: Prentice-Hall, 2001.
[22] P. Kyösti, J. Meinilä, L. Hentilä, X. Zhao, T. Jämsä, C. Schneider, M. Narandzic, M. Milojevic, A. Hong, J. Ylitalo, V.-M. Holappa, M. Alatossava, R. Bultitude, Y. de Jong, and T. Rautiainen, "WINNER II channel models," Eur. Union, WINNER II D1.1.2 V1.1, Tech. Rep. version 1.1, 2007.
[23] *Study Channel Model for Frequencies From 0.5 to 100 GHz (Release 16)*, Standard TR 38.901, v6.1.0, 3GPP, Dec. 2019.
[24] M. Gudmundson, "Correlation model for shadow fading in mobile radio systems," *Electron. Lett.*, vol. 27, no. 23, pp. 2145–2146, Nov. 1991.
[25] K. Siwiak, *Radiowave Propagation and Antennas for Personal Communications*. Norwood, MA, USA: Artech House, 1995.
[26] S. Saunders and A. Aragon-Zavala, *Antennas and Propagation for Wireless Communication System*, 2nd ed. Hoboken, NJ, USA: Wiley, 2007.
[27] J. Monserrat, R. Fraile, D. Calabuig, and N. Cardona, "Complete shadowing modeling and its effect on system level performance evaluation," in *Proc. IEEE Veh. Technol. Conf.*, May 2008, pp. 294–298.
[28] J. Weitzen and T. J. Lowe, "Measurement of angular and distance correlation properties of log-normal shadowing at 1900 MHz and its application to design of PCS systems," *IEEE Trans. Veh. Technol.*, vol. 51, no. 2, pp. 265–273, Mar. 2002.
[29] A. Mishra, *Fundamentals of Cellular Network Planning and Optimisation*, 2nd ed. Hoboken, NJ, USA: Wiley, 2018.
[30] P. Agrawal and N. Patwari, "Correlated link shadow fading in multi-hop wireless networks," *IEEE Trans. Wireless Commun.*, vol. 8, no. 8, pp. 4024–4036, Aug. 2009.
[31] R. Inam, N. Schrammar, K. Wang, A. Karapantelakis, L. Mokrushin, A. V. Feljan, and E. Fersman, "Feasibility assessment to realise vehicle teleoperation using cellular networks," in *Proc. IEEE 19th Int. Conf. Intell. Transp. Syst. (ITSC)*, Nov. 2016, pp. 2254–2260.
[32] S. Neumeier, E. A. Walelgne, V. Bajpai, J. Ott, and C. Facchi, "Measuring the feasibility of teleoperated driving in mobile networks," in *Proc. Netw. Traffic Meas. Anal. Conf. (TMA)*, Jun. 2019, pp. 113–120.
[33] A. Gaber, W. Nassar, A. M. Mohamed, and M. K. Mansour, "Feasibility study of teleoperated vehicles using multi-operator LTE connection," in *Proc. Int. Conf. Innov. Trends Commun. Comput. Eng. (ITCE)*, Feb. 2020, pp. 191–195.
[34] M. Lauridsen, T. Kolding, G. Pocovi, and P. Mogensen, "Reducing handover outage for autonomous vehicles with LTE hybrid access," in *Proc. IEEE Int. Conf. Commun. (ICC)*, May 2018, pp. 1–6.
[35] U. Saeed, J. Hamalainen, E. Mutafungwa, R. Wichman, D. G. González, and M. Garcia-Lozano, "Route-based radio coverage analysis of cellular network deployments for V2N communication," in *Proc. Int. Conf. Wireless Mobile Comput., Netw. Commun. (WiMob)*, Oct. 2019, pp. 1–6.
[36] M. Lauridsen, L. C. Gimenez, I. Rodriguez, T. B. Sorensen, and P. Mogensen, "From LTE to 5G for connected mobility," *IEEE Commun. Mag.*, vol. 55, no. 3, pp. 156–162, Mar. 2017.
[37] S. Shetty, S. Lackovic, and S. Z. Pilinsky, "4G coverage analysis of croatian main roads," in *Proc. Int. Symp. ELMAR*, Sep. 2017, pp. 129–132.
[38] "The 2019 mobile network in Spain," Umlaut, Aachen, Germany, Tech. Rep., 2020.
[39] W. Navidi, *Statistics for Engineers and Scientists*. New York, NY, USA: McGraw-Hill, 2004.

MATÍAS TORIL received the M.S. degree in telecommunication engineering and the Ph.D. degree from the University of Málaga, Spain, in 1995 and 2007, respectively. Since 1997, he has been a Lecturer with the Communications Engineering Department, University of Málaga, where he is currently a Full Professor. He has coauthored more than 150 publications in leading conferences and journals and eight patents owned by Nokia and Ericsson. His current research interests include self-organizing networks, radio resource management, and data analytics.

VOLKER WILLE received the B.S. degree from the University of Applied Sciences and Arts of Hannover, Hannover, Germany, in 1991, and the Ph.D. degree from the University of Glamorgan, Cardiff, U.K., in 1995. He was an Intern with Bell Communications Research, Morristown, NJ, USA. He is currently with Nokia, Huntingdon, U.K., where he is involved in the optimization of cellular networks.

SALVADOR LUNA-RAMÍREZ received the M.S. degree in telecommunication engineering and the Ph.D. degree from the University of Málaga, Spain, in 2000 and 2010, respectively. Since 2000, he has been with the Communications Engineering Department, University of Málaga, where he is currently an Associate Professor. His research interests include self-optimization of mobile radio access networks and radio resource management.

MARIANO FERNÁNDEZ-NAVARRO received the M.S. degree in telecommunication engineering from the Polytechnic University of Madrid, in 1988, and the Ph.D. degree from the University of Málaga, in 1999. He has been the Staff of the Communications Engineering Department, University of Málaga, since 1992, after three years as a Design Engineer with Fujitsu Spain S.A. His research interests include optimization of radio resource management for mobile networks and location-based services and management.

FERNANDO RUIZ-VEGA received the M.S. degree in telecommunication engineering from the University of Málaga, Spain, in 1994. After working in CETECOM testing laboratory with type-approval test systems for communication equipment, he joined the Communications Engineering Department, University of Málaga, where, in 2001, he became an Associate Professor. In 1995, he was a Visiting Researcher with the Department of Electrical Engineering and Electronics, University of Liverpool, Liverpool, U.K. From 2000 to 2002, he took part in the Nokia Mobile Communications Competence Centre, Málaga, Spain. His research interests include mobile radio propagation channel characterization and emulation.